

# Broadband Active Imaging Method Using Auto-Correlation Pulse Response

# Hiroyasu SATO <sup>1</sup>, Kunio SAWAYA <sup>1</sup>

<sup>1</sup> Graduate School of Engineering, Tohoku University  
Aza-Aoba 05, Aramaki, Aobaku, Sendai, 980-8579, Japan  
E-mail: {sahiro, sawaya}@ecei.tohoku.ac.jp

## Abstract

A method for broadband active imaging using the autocorrelation pulse (ACP) response is proposed to realize a low cost real-time imaging system constructed by power detector array. In this method, swept continuous waves in a broad frequency range are transmitted to the scatterer and the received power spectrum obtained by means of the squared detection of scattered waves is transformed into ACP response by using the Inverse Fourier Transformation (IFT). Then ACP response is used for the imaging of objects. ACP response can be obtained by using only the magnitude of scattered waves, but it includes non-physical (false) response. It is shown theoretically and experimentally that a strong couple between the transmitting and receiving antennas yield the reduction of the false pulses.

## 1. INTRODUCTION

Recently, many kinds of applications using EM pulse or broadband frequency range have been considered by many researchers so far. In the field of measurements, it is possible to realize high resolution pulse radars using broadband frequency applicable to the imaging of objects such as through walls, in concrete, under ground, concealed weapons inside the clothes etc.

When swept continuous signal in a broad frequency instead of pulse is used for pulse radar, RF mixer, broadband 90° phase-shifter, RF switches and fast analog/digital converters are required to measure the complex scattered field but they are not available with low cost.

In our previous paper [1], high gain antipodal Fermi antenna (APFA) which is one of the tapered slot antenna with the combination of antipodal feeding section and Fermi-Dirac taper section has been proposed and applied to the through-wall imaging of metallic objects by the scanning transmitting and receiving APFAs as a quasi-monostatic radar [2].

In this paper, an active imaging method using the autocorrelation pulse (ACP) response is proposed to realize a low cost real-time imaging system. In this method, a quasi-monostatic radar composed of transmitting and receiving APFAs is used.

Swept continuous waves in a broad frequency range are transmitted to the scatterer and the scattered field is received and detected as square DC voltage corresponding to the power of scattered waves. The power spectrum is transformed into

the autocorrelation function by using IFT, which is used for the imaging of objects.

The autocorrelation pulse (ACP) response can be obtained by using only the magnitude of scattered waves which means that the DC switching by low cost multiplexer is applicable for the purpose of real-time imaging. ACP response includes non-physical response which does not appear in the “real” pulse response obtained by using the complex value of scattered waves. It is shown theoretically and experimentally that a strong couple between the transmitting and receiving antennas yield the reduction of the false pulses.

## 2. THEORETICAL FORMULATIONS

Let us consider a quasi-monostatic broadband radar and an pulse response  $f(t)$  scattered by objects

$$f(t) = \sum_{l=1}^L \alpha_l \delta(t - t_l) \quad (1)$$

where  $\alpha_l$  and  $t_l$  denote magnitude and delay time of each pulse, respectively, and  $L$  is corresponding to the number of scatterers or the number of multiple scattered waves. The autocorrelation function  $C(t)$  is defined by

$$C(t) = \int_{-\infty}^{\infty} f(\tau) f(t - \tau) d\tau = \int_{-\infty}^{\infty} |F(\omega)|^2 e^{-j\omega t} d\omega. \quad (2)$$

Substituting Eq. (1) into Eq. (2) and deviding into three terms of  $i = j$  and  $i = 1, j = 2, 3, \dots, L$  and otherwise,  $C(t)$  is given by

$$\begin{aligned} C(t) &= \sum_{i=1}^L \sum_{j=1}^L \alpha_i \alpha_j \delta(t - t_j + t_i) \\ &= \left( \sum_{l=1}^L \alpha_l^2 \right) \delta(t) \\ &+ \sum_{j=2}^L \alpha_1 \alpha_j \delta(t - t_j + t_1) \\ &+ \sum_{i=2}^{L-1} \sum_{j=i+1}^L \alpha_i \alpha_j \delta(t - t_j + t_i). \end{aligned} \quad (3)$$

Delay times of the first and the second term of  $C(t - t_1)$  are corresponding to that of a pulse response  $f(t)$  and we call them as “real” ACP response. Also it is noted that the third

term with delay time of  $t_j - t_i + t_1$  does not correspond to delay time of  $f(t)$  and we call it as “false” ACP response. The maximum number of false ACP response is given by  $N_F = (L-1)P_2/2 = (L-1)(L-2)/2$ .

When the magnitude of the pulse  $\alpha_1$  corresponding to  $t_1$  is much greater than the magnitudes of other pulses  $\alpha_l$  ( $l = 2, \dots, L$ ), we can reduce the false ACP response as can be seen in Eq. (3). The largest pulse is usually generated by the direct coupling between the transmitting and receiving antennas.

### 3. UTILIZATION OF SINGLE PEAKED MUTUAL COUPLING PULSE RESPONSE AS $\alpha_1$

In order to control the value of  $\alpha_1$ , a quasi-monostatic radar using closely located transmitting and receiving antennas is employed. The mechanism of mutual coupling is complicated and is usually desired to decrease so as not to affect the performance of antennas, however, it plays an important role in the proposed method.

Two element APFAs previously proposed in [1-2] are used as a quasi-monostatic radar as shown in Fig. 1. The VSWR of APFA is less than 2 in the frequency range of 6-18 GHz and the gain is 14 dBi at the center frequency of 10 GHz with almost uniform frequency characteristics.

Fig. 1 shows the mutual coupling between two APFAs when the spacing is  $d_{21} = 10$  mm and 60 mm. The values of mutual coupling are less than -20dB for both cases in the frequency range of higher than 7 GHz and quite small values are obtained in the case of  $d_{21} = 60$  mm.

Fig. 2 shows the time domain mutual coupling response obtained by IFT of complex values of  $S_{21}$  by using hanning window function in the frequency region of 6-18 GHz. Band limited pulse response becomes a burst pulse response and only the envelope obtained by Hilbert transformation is plotted in Fig. 3. In the case of  $d_{21} = 10$  mm, almost single pulse response of the direct coupling is observed with small distortion and it can be used as a pulse response corresponding to  $\alpha_1$ .

### 4. APPLICATION TO CIRCULAR-SCAN IMAGING

Let us consider a scattering object located near the origin  $O$  of the cylindrical coordinate system as shown in Fig. 3, where  $P(\rho', \phi')$  denotes the position of APFA and  $Q(\rho, \phi)$  denotes the scattering point in a region of  $\rho \leq \rho'$ . The cross section of scattering object composed of a metal plate and a metal cylinder placed in a cardboard box is also shown in Fig. 3.

The transmitting and receiving APFAs are scanned along a circle of radius  $\rho' = 400$  mm with an angular step of  $\Delta\phi' = 6^\circ$ . A pulse response  $f(\phi', t)$  scattered at the point  $Q$  has a delay time corresponding to a distance  $2\overline{PQ}$ . The imaging function  $u(\rho, \phi)$  is obtained by superposition of  $f(\phi', t)$

$$u(\rho, \phi) = \int_0^{2\pi} f(\phi', \frac{2\overline{PQ}}{c}) d\phi' \quad (4)$$

where  $\overline{PQ} = \{\rho^2 + \rho'^2 - 2\rho\rho' \cos(\phi - \phi')\}^{\frac{1}{2}}$ . The results by using above equation are already reported in [3] and we used

the imaging function  $u^{ACP}(\rho, \phi)$  expressed by superposition of ACP response  $C(\phi', t - t_1)$

$$u^{ACP}(\rho, \phi) = \int_0^{2\pi} C(\phi', \frac{2\overline{PQ}}{c}) d\phi' \quad (5)$$

First, the vector network analyzer is used for measuring complex  $S_{21}$  in the frequency domain to obtain  $f(t)$ .  $|S_{21}|^2$  is used to obtain  $C(t)$ . The hanning window function in the frequency region of 6-18 GHz is used for both cases.

Fig. 4 shows the imaging function  $u^{ACP}(\rho, \phi)$  when the spacing is  $d_{21} = 60$  mm, 30 mm and 10 mm. In the case of  $d_{21} = 60$  mm, image of the scattering objects can not be observed and strong image appears near the region of  $\rho = 300$  mm and  $|\phi| < 30^\circ$ . On the other hand, clearer image of objects are obtained as the spacing of antennas decrease.

Fig. 5 show the pulse response  $f(t)$  and ACP response  $C(t - t_1)$  when the incident angle of  $\phi = 0^\circ$ . Scattered waves by the cardboard box, the metal cylinder and the metal plate are observed in the pulse response  $f(t)$  at the same time delays of  $t_2, t_3$  and  $t_4$  for the case of three spacings. However, in ACP response  $C(t - t_1)$  of  $d_{21} = 60$  mm, dominant response is observed around 3 ns which is corresponding to the false ACP pulse with time delay of  $t_4 - t_3 + t_1$ . Also the false ACP responses at  $t_4 - t_2 + t_1 = 3.4$  ns and  $t_3 - t_2 + t_1 = 2.4$  ns are observed. However, these false ACP response are reduced as  $d_{21}$  decrease which is considered that the magnitude of mutual coupling pulse  $\alpha_1$  with time delay of  $t_1$  becomes large compared with the magnitude of scattered waves at time delays of  $t_2, t_3$  and  $t_4$  conforming the reduction method of the false pulses.

Finally, an experiment using diode detector connected to the receiving antenna was performed as shown in Fig. 6. The autocorrelation function  $C(t)$  is obtained by IFT of the power spectrum. Fig. 7 shows the imaging function  $u^{ACP}(\rho, \phi)$  when the spacing is  $d_{21} = 30$  mm. It is observed that a distribution of  $u^{ACP}(\rho, \phi)$  similar to Fig. 4(b) is obtained.

### 5. CONCLUSION

An active imaging method using ACP response has been proposed for the purpose to realize a low cost real-time imaging system. A method to reduce the magnitude of false pulses which appears in ACP response has been also proposed. Experiment of circular-scan imaging has been performed and the validity of the proposed method is confirmed. The real-time imaging by the array of APFA is a remaining subject.

### REFERENCES

- [1] Y. Takagi, H. Sato, Y. Wagatsuma, K. Sawaya and K. Mizuno, “Study of high gain and broadband antipodal Fermi antenna with corrugation,” International Symposium on Antennas and Propagation (ISAP2002), vol. 1, pp. 69-72, Sendai, Japan, 2004.
- [2] H. Sato, Y. Takagi, Y. Wagatsuma, K. Mizuno, and K. Sawaya, “Time Domain Characteristics of Broadband Antipodal Fermi Antenna And Its Application To Through-wall Imaging,” International Symposium on Antennas and Propagation (ISAP2005), vol. 1, pp. 338-390, Seoul, Korea, 2005.
- [3] H. Sato, K. Nakanishi and K. Sawaya, “Experimental Study of Circular-Scan Time-Domain Active Imaging by Using Broadband Antipodal Fermi Antenna,” 2006 IEEE AP-S International Symposium, Albuquerque, NM, pp. 901-904, July 2006.

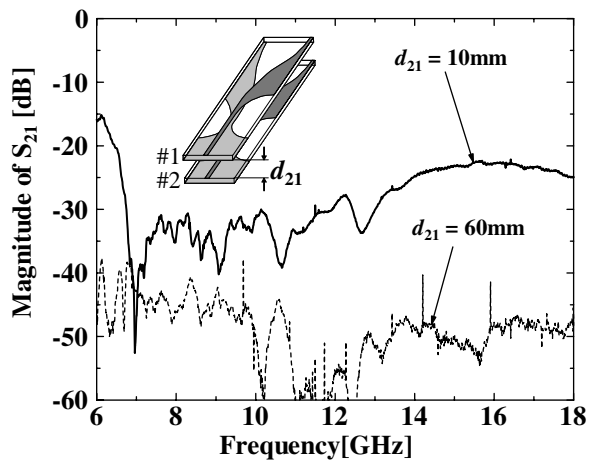


Fig. 1: Mutual coupling between two APFAs.

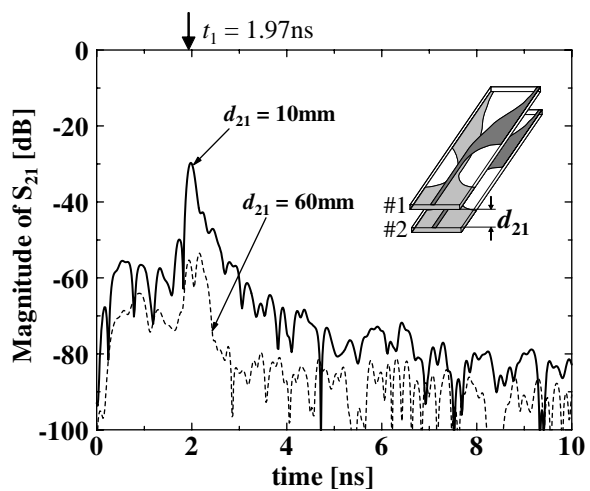


Fig. 2: Pulse response between two APFAs.

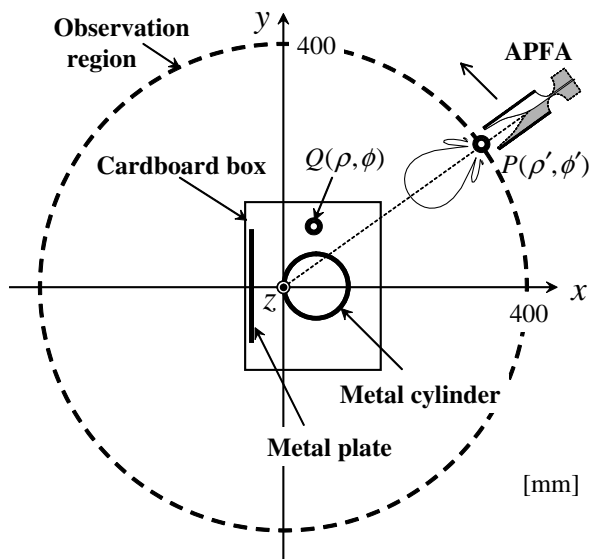
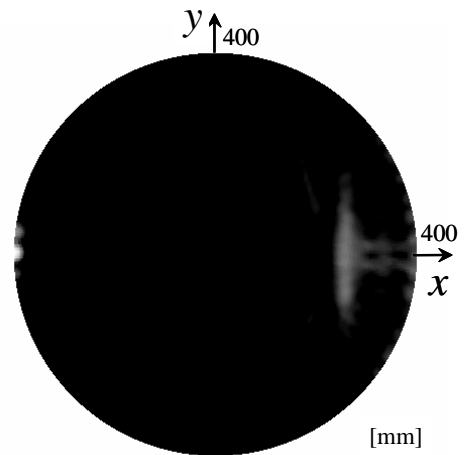
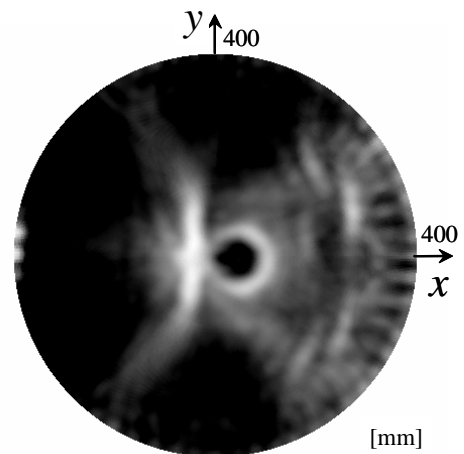


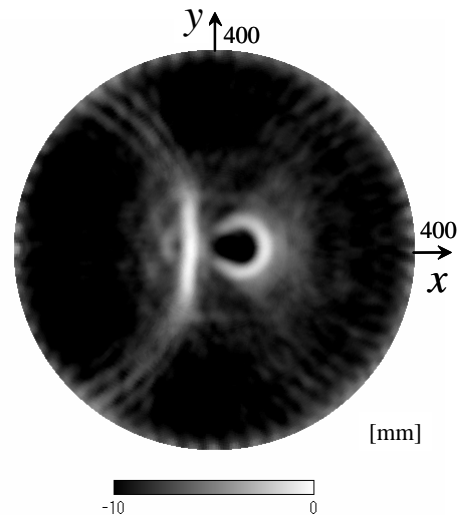
Fig. 3: Circular-scan imaging of scattering objects.



(a)  $d_{21} = 60$  mm

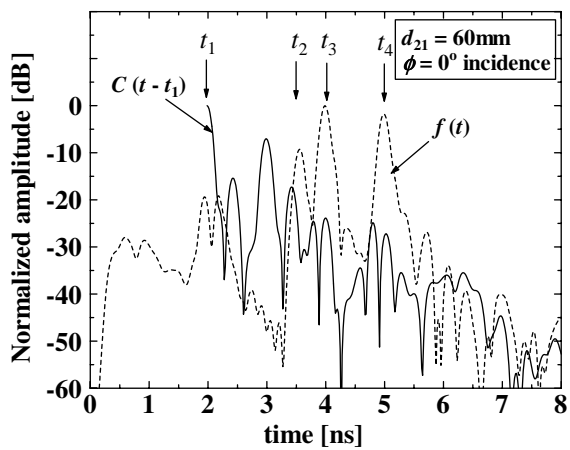


(b)  $d_{21} = 30$  mm

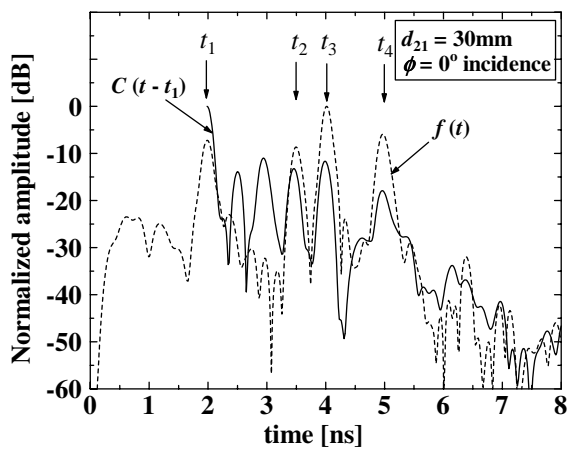


(c)  $d_{21} = 10$  mm

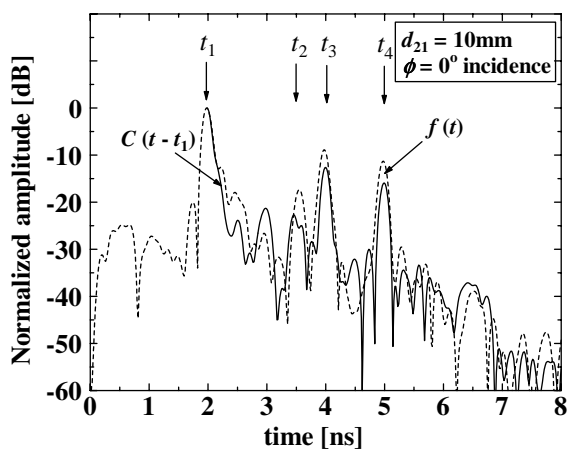
Fig. 4: Imaging function  $u^{ACP}(\rho, \phi)$ . Normalized by maximum value.



(a)  $d_{21} = 60$  mm



(b)  $d_{21} = 30$  mm



(c)  $d_{21} = 10$  mm

Fig. 5: Pulse response  $f(t)$  and ACP response  $C(t - t_1)$  in case when incident angle  $\phi = 0^\circ$ . Normalized by maximum value for each case.

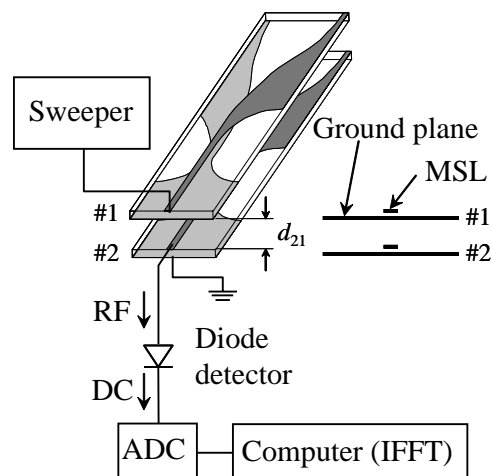


Fig. 6: Two element APFAs and experimental setup.

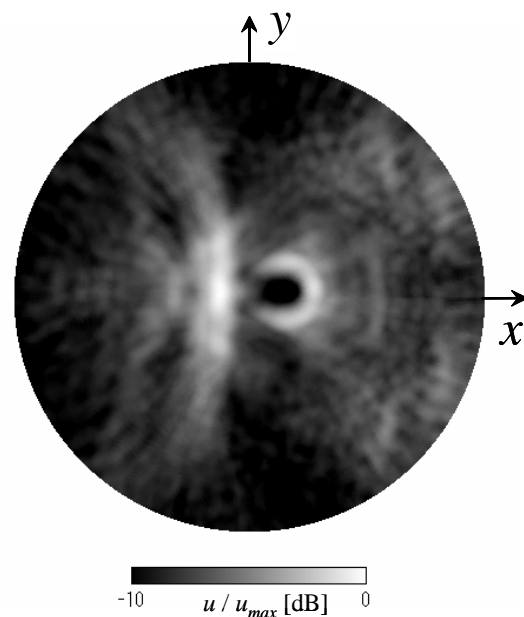


Fig. 7: Imaging function when frequency response of detected voltage is used to obtain ACP response.